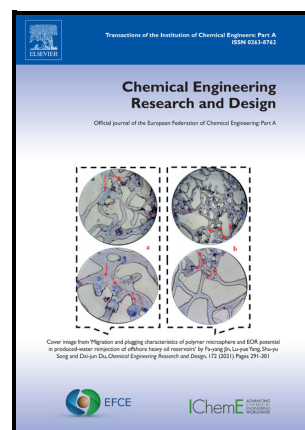


Comparison of analytical film theory and a numerical model for predicting concentration polarisation in membrane gas separation

K. Foo, Y.Y. Liang, P.S. Goh, A.L. Ahmad, D.K. Wang, D.F. Fletcher



PII: S0263-8762(22)00358-6

DOI: <https://doi.org/10.1016/j.cherd.2022.07.014>

Reference: CHERD5070

To appear in: *Chemical Engineering Research and Design*

Received date: 30 May 2022

Revised date: 8 July 2022

Accepted date: 13 July 2022

Please cite this article as: K. Foo, Y.Y. Liang, P.S. Goh, A.L. Ahmad, D.K. Wang and D.F. Fletcher, Comparison of analytical film theory and a numerical model for predicting concentration polarisation in membrane gas separation, *Chemical Engineering Research and Design*, (2022) doi:<https://doi.org/10.1016/j.cherd.2022.07.014>

This is a PDF file of an article that has undergone enhancements after acceptance, such as the addition of a cover page and metadata, and formatting for readability, but it is not yet the definitive version of record. This version will undergo additional copyediting, typesetting and review before it is published in its final form, but we are providing this version to give early visibility of the article. Please note that, during the production process, errors may be discovered which could affect the content, and all legal disclaimers that apply to the journal pertain.

© 2022 Published by Elsevier.

Comparison of analytical film theory and a numerical model for predicting concentration polarisation in membrane gas separation

K. Foo^a, Y. Y. Liang^{a}, P. S. Goh^b, A. L. Ahmad^c, D. K. Wang^d, D. F. Fletcher^d*

^aCollege of Engineering, Universiti Malaysia Pahang, Lebuhraya Tun Razak, 26300 Gambang, Kuantan, Pahang, Malaysia

^bAdvanced Membrane Technology Research Centre (AMTEC), School of Chemical and Energy Engineering, Faculty of Engineering, Universiti Teknologi Malaysia (UTM), 81310 Skudai, Johor, Malaysia

^cSchool of Chemical Engineering, Engineering Campus, Universiti Sains Malaysia, 14300 Nibong Tebal, Seberang Prai Selatan, Pulau Pinang, Malaysia

^dThe University of Sydney, School of Chemical and Biomolecular Engineering, NSW 2006, Australia

* Corresponding author. Tel.: +609 549 2859. E-mail: yongyeow.liang@ump.edu.my

Abstract

Accurate prediction of the concentration polarisation (CP) effect is very important in the design of an efficient membrane-based gas separation process. This study analyses the reliability of analytical film theory (FT) for evaluating the performance of gas separation membranes in terms of CP and flux. The analytical model is compared against a more rigorous numerical model developed by using Computational Fluid Dynamics (CFD) for various operating variables. The results show that the FT prediction is less accurate at high CP conditions when gas permeation through the membrane increases, due to higher permeance selectivity and pressure ratio. Hence, the results suggest that FT is not recommended for membranes with high permeance or high-pressure conditions. Given that the typical range of feed composition and temperature has little impact on fluid properties (i.e., gas diffusion coefficient, densities, and viscosities), the resulting CP does not vary much and hence both FT and CFD models predict a similar CP. The analysis also suggests that the FT model is more accurate in predicting CP in the region closer to the membrane entrance. Overall, the analytical film theory serves as a reliable approximation in membrane gas applications under low CP at high crossflow and low flux conditions.

Keywords:

CFD, membrane gas separation, concentration polarisation, analytical film theory, gas permeation flux

1 Introduction

Concentration polarisation (CP) is one of the critical problems associated with membrane separation processes. CP occurs when the gradual accumulation of the rejected species takes place near the membrane surface due to the selective permeability of membranes (Al-Obaidi and Mujtaba, 2016; Matthiasson and Sivik, 1980). The increased CP would eventually reduce the driving force between the feed and permeate sides of the membrane, thus decreasing the membrane overall performance. In membrane gas separations, the phenomenon occurs when the concentration of the less permeable species increases in the boundary layer adjacent to the membrane surface as a result of rapid permeation of the more permeable species through the membrane (Baker, 2004). Early studies have confirmed that the polarisation effects cannot be neglected for gas separations, especially for membranes with high permeability (Bhattacharya and Hwang, 1997; Chen et al., 2011; Chen et al., 2012; He et al., 1999; Lüdtke et al., 1998; Mourgues and Sanchez, 2005; Takaba and Nakao, 2005; Zhang et al., 2006). Therefore, CP prediction is an important aspect in designing membrane-based gas separation processes and evaluating the performance of membranes.

Early theoretical models, such as the film theory (FT), were developed to describe CP phenomena by assuming the formation of a boundary layer of thickness (δ) associated with impermeable membrane walls (Baker, 2004; Michaels, 1968; Probstein et al., 1977; Zydney, 1997). In addition, the analytical model also simplifies the mass transport problem by assuming a uniform concentration along the membrane channel, such that the boundary layer thickness is independent of the transverse flow field (permeate flux). Nevertheless, no study up to now has discussed the accuracy of the film theory model against numerical simulations for describing CP in membrane-based gas separation.

Hence, this paper aims to analyse the reliability of analytical film theory and its limitations for evaluating the performance of gas separation membranes. The analytical model is compared against a more rigorous numerical model developed using computational fluid dynamics (CFD), which solves the flow and continuity equations for the gas separation system by taking into account the coupling of momentum and mass transport. The calculations are performed for typical CO₂/CH₄ gas separation (Feng et al., 2021; Liang et al., 2018; Liang et al., 2017), and the performance is analysed in terms of CP and flux by considering the effects of varying hydraulic Reynolds number (Re_h), membrane selectivity, feed composition, temperature, as well as pressure ratio in the membrane system.

2 Methodology

2.1 Theoretical background of CP analytical model by film theory

Current commercial membrane gas separation processes mainly use dense polymeric membranes. The separation of gas mixtures through the dense membrane film is generally described by the solution-diffusion mechanism, where a gas component dissolves into the membrane material and then permeates through the dense film down a concentration gradient (Baker, 2004). The transport of gas components within the boundary layer at any point in the membrane feed channel can be expressed by using Fick's law as follows:

$$\rho j_f w_i - \rho D \frac{\partial w_i}{\partial y} = \rho j_p w_{i,p} \quad (1)$$

where ρ is the density, w_i is the mass fraction of gas species i , D is the diffusion coefficient, j_f and j_p are the volume fluxes of gas ($\text{m}^3 \text{m}^{-2} \text{s}^{-1}$) on the feed and permeate sides of the membrane, respectively.

In gases, the volume fluxes on the feed and permeate sides of the membrane are not the same. Nevertheless, the gas volume fluxes can relate with each other by correcting for the feed and permeate pressures, p_f and p_p on each membrane side as follows:

$$j_f p_f = j_p p_p \quad (2)$$

This gives

$$j_f \frac{p_f}{p_p} = j_f \varphi = j_p \quad (3)$$

where φ is the pressure ratio $\left(\frac{p_f}{p_p}\right)$ of the membrane system. Using the definition of pressure ratio to relate the gas volume fluxes on each membrane side in equation (1) gives the following expression

$$-\rho D \frac{\partial w_i}{\partial y} = \rho j_f (\varphi w_{i,p} - w_i) \quad (4)$$

The mass balance equation (4) can be integrated over the boundary layer thickness (δ) to give a concentration polarisation equation (Brian, 1965) as follows:

$$\frac{w_{i,o}/\varphi - w_{i,p}}{w_{i,b}/\varphi - w_{i,p}} = \exp\left(\frac{j_f \delta}{D}\right) \quad (5)$$

Alternatively, the concentration terms in equation (5) can be replaced using the membrane enrichment terms, E and E_o . The enrichment terms represent the factors which determine the magnitude of concentration polarisation based on the difference in gas permeabilities (Baker, 2004). As the difference in gas permeabilities increases, the membrane enrichment terms increase, resulting in larger concentration gradients and thus higher CP. The enrichment terms for gases are generally expressed as volume fractions in terms of the pressure ratio (ϕ), such that

$$E = \frac{w_{i,p}}{w_{i,b}} \cdot \phi \quad (6)$$

Excluding the presence of a boundary layer, E_o is expressed as

$$E_o = \frac{w_{i,p}}{w_{i,o}} \cdot \phi \quad (7)$$

It must be noted that both enrichment terms for CO₂ are larger than one because the membrane selectively permeates the gas component. Substituting the enrichment terms into equation (5) gives

$$\frac{1-1/E_o}{1-1/E} = \exp\left(\frac{j_f \delta}{D}\right) \quad (8)$$

The extent of concentration polarisation is measured by the magnitude of the ratio between the permeate concentration at the membrane surface ($w_{i,o}$) compared with the bulk concentration ($w_{i,b}$). Hence, CP effect becomes significantly important when the CP modulus ($\gamma = w_{i,o}/w_{i,b}$) deviates from one. In this case, the CP modulus is represented by the concentration gradient of the more permeable CO₂ gas component. By using the definitions of E and E_o , the CP modulus can be expressed as

$$\gamma = \frac{E}{E_o} = \frac{w_{i,o}}{w_{i,b}} = \frac{\exp(j_f \delta / D)}{1 + E_o [\exp(j_f \delta / D) - 1]} \quad (9)$$

Later the gas volume flux is predicted by CFD calculations and used as an input in CP prediction for the analytical solution as in equation (9). For a fully developed laminar flow in a narrow rectangular channel with soluble walls (Probstein, 1989), the boundary layer thickness can be expressed as

$$\frac{\delta(x)}{x} = 1.475 \left(\frac{h}{x} \right)^{2/3} \left(\frac{D}{u_{\max} h} \right)^{1/3} \quad (10)$$

where x is the longitudinal coordinate, h is the channel half-height, and u_{\max} is the maximum crossflow velocity at the centre of channel. The equations and theories used for estimating gas mixture properties are listed in Table 1:

Table 1: Mathematical formulation used for estimation of gas mixture properties.

Gas properties	Theory of formula	Mathematical equation
Diffusion coefficient, D ($\text{m}^2 \text{s}^{-1}$)	Chapman and Enskog theory (Cussler, 1997).	$D = \frac{1.86 \times 10^{-3} T^{3/2} (1/M_i + 1/M_j)^{1/2}}{p \sigma_{ij}^2 \Omega}$
Density of gas mixture, ρ_{mix} (kg m^{-3})	Ideal gas law (Moran and Shapiro, 1988).	$\rho_{\text{mix}} = \frac{1}{\sum \left(\frac{w_i}{\rho_i} \right)_n}$
Dynamic viscosity of gas mixture, μ_{mix} ($\text{kg m}^{-1} \text{s}^{-1}$)	Wilke correlation (Wilke, 1950).	$\mu_{\text{mix}} = \frac{\sum (\mu_i n_i \sqrt{M_i})}{\sum (n_i \sqrt{M_i})}$

2.2 Flux calculations for membrane gas separation

In gas separation, the driving force across the membrane is driven by the partial pressure difference of the gas component across the membrane, which can be expressed as follows:

$$J_i = P_i (p_{i,o} - p_{i,p}) \quad (11)$$

where J_i is the mass flux of gas species i ($\text{kg m}^{-2} \text{s}^{-1}$), P_i is the gas permeance, $p_{i,o}$ and $p_{i,p}$ are the partial pressures of the gas species on the feed and permeate sides of the membrane, respectively. Note that the total gas pressures on a membrane side (either feed or permeate) are the summation of gas partial pressures for a mixture of species i and j , respectively. The partial pressures are related to the mole fractions of the gas species on both sides of the membrane and can be calculated as

$$n_{i,o} = \frac{p_{i,o}}{p_o} \quad n_{i,p} = \frac{p_{i,p}}{p_p} \quad (12)$$

Hence, the flux equation (11) can be rewritten as

$$J_i = P_i (n_{i,o} p_o - n_{i,p} p_p) \quad (13)$$

and $n_{i,p}$ is determined using the following expression by relating the concentration of gas species i on both sides of the membrane (i.e. feed and permeate sides) (Baker, 2004):

$$n_{i,p} = \frac{\varphi}{2} \left[n_{i,o} + \frac{1}{\varphi} + \frac{1}{\alpha - 1} - \sqrt{\left(n_{i,o} + \frac{1}{\varphi} + \frac{1}{\alpha - 1} \right)^2 - \frac{4\alpha n_{i,o}}{(\alpha - 1)\varphi}} \right] \quad (14)$$

where α is the membrane selectivity. Membrane selectivity (α) is a quantification of the ability of a membrane to separate two gases, i and j , and can be expressed as

$$\alpha = \frac{P_i}{P_j} \quad (15)$$

Table 2 summaries the differences between the numerical solution using the CFD approach and the film theory (FT) approximation as follows:

Table 2: Summary of the differences between the numerical approach and the film theory approximation.

Description	Numerical solution (CFD simulation)	FT approximation	Significance and source of difference
Concentration polarisation (CP) and permeate flux	Can be calculated directly by solving the mass transport of gas component within the local boundary layer using Fick's law.	Requires gas concentration and flux input data from either experimental or numerical simulation for calculations of CP and permeate flux.	The effect of varying solute permeation on CP for FT approximation is not considered.
Flow profiles	Resolves the local velocity distribution within the fluid domain.	The local velocity profiles cannot be predicted directly.	CFD requires higher computational effort.

2.3 Description of numerical model by CFD

Figure 1 shows a schematic diagram of the 2D CFD fluid domain used for modelling CO₂/CH₄ gas separation in this paper. An empty rectangular channel is constructed for the fluid domain (Figure 1), which is a simplified geometry of a hollow fibre membrane channel (Liang et al., 2018). A membrane length (L_m) of 1 m is used for the fluid domain as it is the typical dimension used in commercial hollow fibre gas separation modules (Ahmad et al., 2015). The length of the entrance region is set as one-fifth of the membrane length ($\frac{1}{5} \times L_m$), and it is doubled for the exit region ($2 \times$ entrance length). These regions are located at each end of the membrane channel to avoid the flow solution being affected by both inlet and outlet boundary conditions (see Figure 1) (Schwinge et al., 2002a, b).

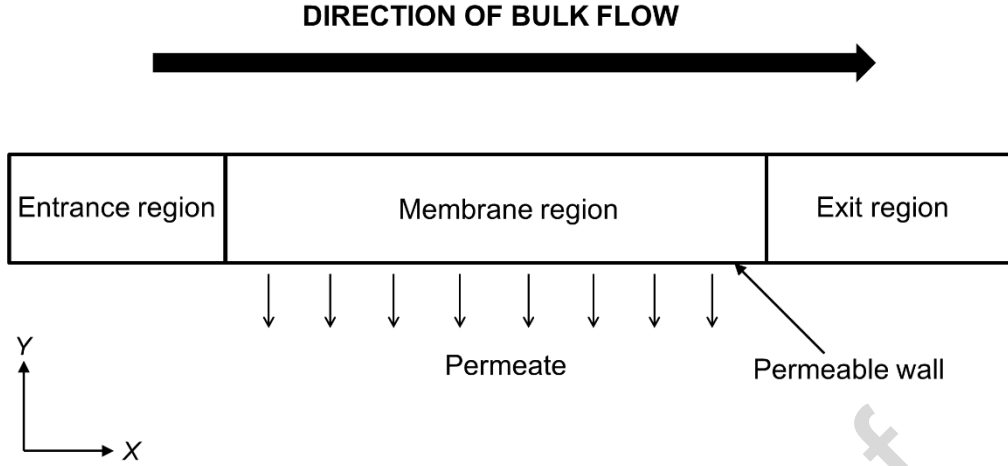


Figure 1: Schematic diagram of CFD fluid domain (not to scale) for modelling of a gas separation feed channel.

2.3.1 Boundary conditions

The present study employs the commercial CFD code, ANSYS CFX-18.2 for simulating an isothermal two-dimensional (2D) flow with constant Newtonian fluid properties inside an empty rectangular channel (Fletcher and Wiley, 2004). The steady-state simulations are performed with negligible gravitational effects and the binary gas mixture (i.e. CO₂ and CH₄ gas) treated as an incompressible fluid (Fletcher and Wiley, 2004; Wiley and Fletcher, 2003). The governing Navier-Stokes equations are therefore, given as in equations (16) to (18), while the mass transport equation for gas species i is expressed in the form of equation (19) as follows:

$$\frac{\partial u}{\partial x} = -\frac{\partial v}{\partial y} \quad (16)$$

$$\rho \frac{\partial u}{\partial t} + \rho \left(u \frac{\partial u}{\partial x} + v \frac{\partial u}{\partial y} \right) = \mu \left(\frac{\partial^2 u}{\partial x^2} + \frac{\partial^2 u}{\partial y^2} \right) - \frac{\partial p}{\partial x} \quad (17)$$

$$\rho \frac{\partial v}{\partial t} + \rho \left(u \frac{\partial v}{\partial x} + v \frac{\partial v}{\partial y} \right) = \mu \left(\frac{\partial^2 v}{\partial x^2} + \frac{\partial^2 v}{\partial y^2} \right) - \frac{\partial p}{\partial y} \quad (18)$$

$$\frac{\partial w_i}{\partial t} + u \frac{\partial w_i}{\partial x} + v \frac{\partial w_i}{\partial y} = D \left(\frac{\partial^2 w_i}{\partial x^2} + \frac{\partial^2 w_i}{\partial y^2} \right) \quad (19)$$

The high-resolution schemes were chosen for solving the partial differential equations (16) to (19) to reduce numerical diffusion. All steady-state simulations are considered to have converged once the RMS errors for residuals drop below 10^{-10} .

The local mass fraction of gas species i and pressure at any point of the membrane wall can be obtained directly from CFD calculations. A parabolic velocity profile is specified

at the feed inlet, whereas the outlet boundary is set to zero relative pressure. The top surface and other non-membrane channel walls, i.e., entrance and exit region walls, are treated as no-slip walls with zero mass flux condition. Table 3 summarises the mathematical expressions used for the boundary conditions specified at different locations of fluid domain boundaries.

Table 3: Mathematical expressions for boundary conditions of CFD model at different locations.

Boundary location	Boundary condition	Mathematical expression
Inlet	Specified parabolic velocity profile (u_{b0}) and concentration profile (w_{b0}).	$u_{b0} = 6u_{avg} (y / h_{ch}) [1 - (y / h_{ch})]$ $w_{b0} = w_{i,b}$
Outlet	Specified zero average reference pressure coupled with no-slip and zero mass flux condition.	$\frac{\partial w}{\partial x} = 0, \quad P = P_{out}$
Membrane bottom wall	Specified fluid velocity normal to the wall (v_w) based on Fick's law of diffusion (Baker, 2004).	$v_w = \frac{J_p}{\rho}$
Symmetry plane	Specified zero velocity and concentration gradients in direction normal to plane.	$\frac{\partial \bar{v}}{\partial z} = 0, \quad \frac{\partial w}{\partial z} = 0$
Membrane top surface and non-membrane channel walls	Set as no-slip walls with zero mass flux.	$\bar{v} = 0, \quad \frac{\partial w}{\partial y} = 0$

2.3.2 Assumption and cases

Mesh independence studies are performed for model verification so that any potential source of numerical errors due to inadequate mesh resolution can be excluded. Typically, a grid resolution with a convergence index (GCI) value below 5% is sufficient for verification studies (Fimbres-Weihs and Wiley, 2010; Roache and Knupp, 1993). This was obtained when the fluid domain was discretised with a structured mesh using a minimum element size of 0.2% and a maximum of 1.6% of the membrane channel height, respectively. In addition, a minimum of 10 inflation layers are applied near the membrane surfaces (with the first layer thickness being approximately 0.1% of the membrane channel height) to properly resolve the velocity and concentration boundary layers. Overall, a fluid domain comprising 1.6 million control volumes is used for which the resulting GCI was below 1% for both permeate flux and friction factor.

Once the steady-state simulation has converged, the local variables, i.e., gas permeation flux and CP modulus, are calculated as the area-averaged variables within the membrane region length (L_m) using the following expression:

$$\bar{\phi} = \frac{1}{L_m} \int \phi dL_m \quad (20)$$

Table 4 and Table 5 describe the reference parameters and operating variables used for the typical CO₂/CH₄ gas separation case studies. It is important to note that all operating variables (as in Table 5) are investigated considering other parameters to be the same following the reference case as indicated in Table 4. The permeate pressure (p_p) is set as constant at atmospheric pressure (see Table 4), which is commonly applied in membrane gas separation system (Saedi et al., 2014; White et al., 1995). It should be noted that feed pressure (p_f) is varied based on the value of pressure ratio as in Table 5. The permeance value of CH₄ (P_j) is fixed for all case studies considered (as in Table 4), while the permeance value of CO₂ (P_i) is varied depending on membrane selectivity (α), as indicated in Table 5 (Blinova and Svec, 2012; Cakal et al., 2012; Yu et al., 2022).

Table 4: Reference parameters used for gas separation case studies.

Reference parameters	Value
Permeate pressure, p_p (Pa)	101325
Pressure ratio, $\varphi = p_f / p_p$	15
Membrane selectivity, $\alpha = P_i / P_j$	25
Gas permeance of CH ₄ , P_j (mol m ⁻² s ⁻¹ Pa ⁻¹)	1×10 ⁻¹⁰
Hydraulic diameter, d_h (m)	0.01
Hydraulic Reynolds number, $Re_h = \rho u_{avg} d_h / \mu$	200
Schmidt number, $Sc = \mu / \rho D$	0.66
Feed concentration of CO ₂ , $n_{i,b0}$	0.5
Temperature, T (°C)	25

Table 5: Operating variables used for CO₂/CH₄ gas separation case studies.

Operating variables	Value
Membrane selectivity, $\alpha = P_i / P_j$	10 – 250
Pressure ratio, $\varphi = p_f / p_p$	5 – 65
Hydraulic Reynolds number, $Re_h = \rho u_{avg} d_h / \mu$	100 – 800
Feed concentration of CO ₂ , $n_{i,b0}$	0.05 – 0.9
Temperature, T (°C)	25 – 60

2.3.3 Comparison between CFD model and analytical correlation

In order to ensure model accuracy, the CFD model presented in this study is compared against the hydrodynamics analytical correlation, i.e. Fanning friction factor (f) at

different Reynolds number. The Fanning friction factor calculated by CFD in an empty membrane channel is given as follows (Bird et al., 1960):

$$f = \frac{d_h \Delta p_{ch}}{2 \rho u_{avg}^2 L_m} \quad (21)$$

where d_h is the hydraulic diameter, Δp_{ch} is the channel pressure drop, u_{avg} is the average velocity, and L_m is the membrane length.

For a fully developed laminar flow in 2D rectangular channels without permeation through membrane, the analytical correlation for calculating friction factor is expressed as (Bird et al., 1960):

$$f = \frac{24}{Re} \quad (22)$$

Figure 2 shows that both CFD and analytically calculated friction factors agree well with each other with a maximum percentage difference of 5.6% as Re increases. The friction factor predicted by CFD is consistently smaller compared with that of the analytical correlation (Figure 2). This is because the gas permeation across the membrane in the CFD model causes a reduction of bulk fluid flow in the membrane channel, leading to a decrease in the u -velocity gradient normal to the membrane wall, and hence lower friction factor (Liang et al., 2014; Liang et al., 2016). Figure 2 also shows that the percentage difference in f prediction is larger at smaller Re . This is expected, as the membrane extracts more fluid relative to the bulk flow at a smaller Re . As the main driver of flux enhancement is driven by hydrodynamics, this gives confidence in the CFD model prediction.

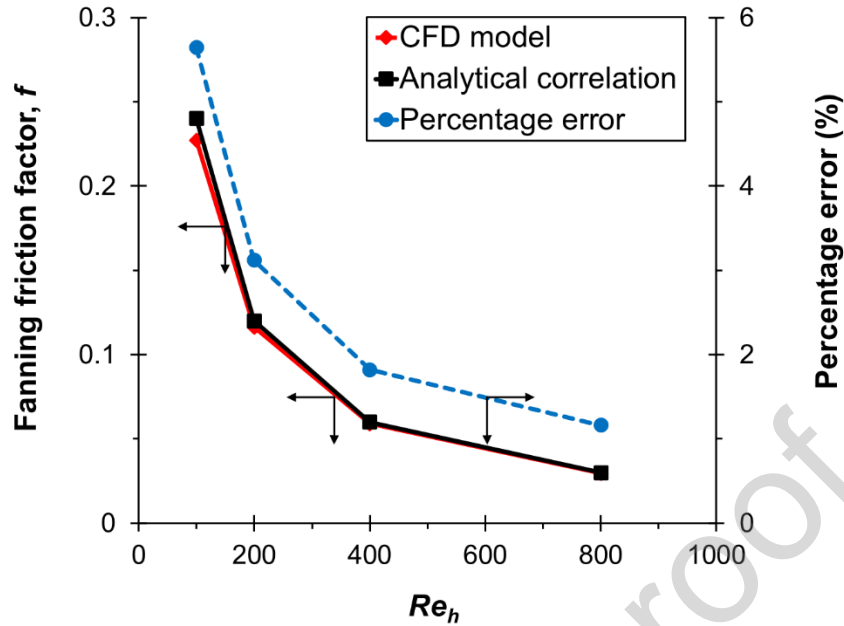


Figure 2: Effect of hydraulic Reynolds number on Fanning friction factor and prediction error (%) between CFD model and analytical correlation.

3 Results and discussion

3.1 Comparison of CP modulus and flux predicted by FT and CFD models

Figure 3 shows that the analytical film theory (FT) model results in a larger area-averaged CP modulus ($\bar{\gamma}$) compared with that predicted using the CFD model, thus indicating that the FT model consistently underestimates CP in the membrane system. As gas permeation increases across the membrane due to higher membrane selectivity (gas permeance) and pressure ratio, this causes a large difference in CP predictions up to 25% between the FT and CFD models (Figure 3a and 3b).

Given that the FT model continues to underpredict CP, this leads to overestimation of gas permeate flux (\bar{J}_{CO_2}) in the membrane system, causing the flux predictions to deviate significantly as selectivity increases, i.e., up to 33% difference between the models (Figure 4a). The significant deviation in predicting CP and flux by the FT model is related to its assumption that the boundary layer thickness does not depend on gas permeation, which undermines the effect of CP on the overall mass transfer performance in the membrane system. Hence, these results suggest that the FT model is not recommended for membranes with high permeance or high-pressure conditions. Note that the pressure ratio implemented in industrial gas applications is not more than 15, due to high cost of the energy requirement

when compared with a slightly increased membrane gas separation rate (Huang et al., 2014). This implies that the present FT model can serve as a reliable prediction as the results agree well with that of CFD for the pressure ratio recommended in practical gas applications, in terms of CP and flux (Figure 3b and Figure 4b).

While the FT prediction is less accurate at high CP conditions typically, the difference in CP and flux predictions between the models, on the other hand, becomes smaller as the flow velocity (or Reynolds number, Re_h) increases, i.e. less than 1% for CP, and 2% for gas permeate flux, as shown in Figure 3c and Figure 4c, respectively. Given that the typical range of feed composition and temperature has little impact on fluid properties, i.e., gas diffusion coefficient, densities, and viscosities (Perry and Green, 2007), the resulting CP and flux do not vary much as well. Therefore, both models predict the membrane performance similarly with the difference in CP and flux predictions is not more than 3% (Figure 3d and 3e) and 6% (Figure 4d and 4e), respectively.

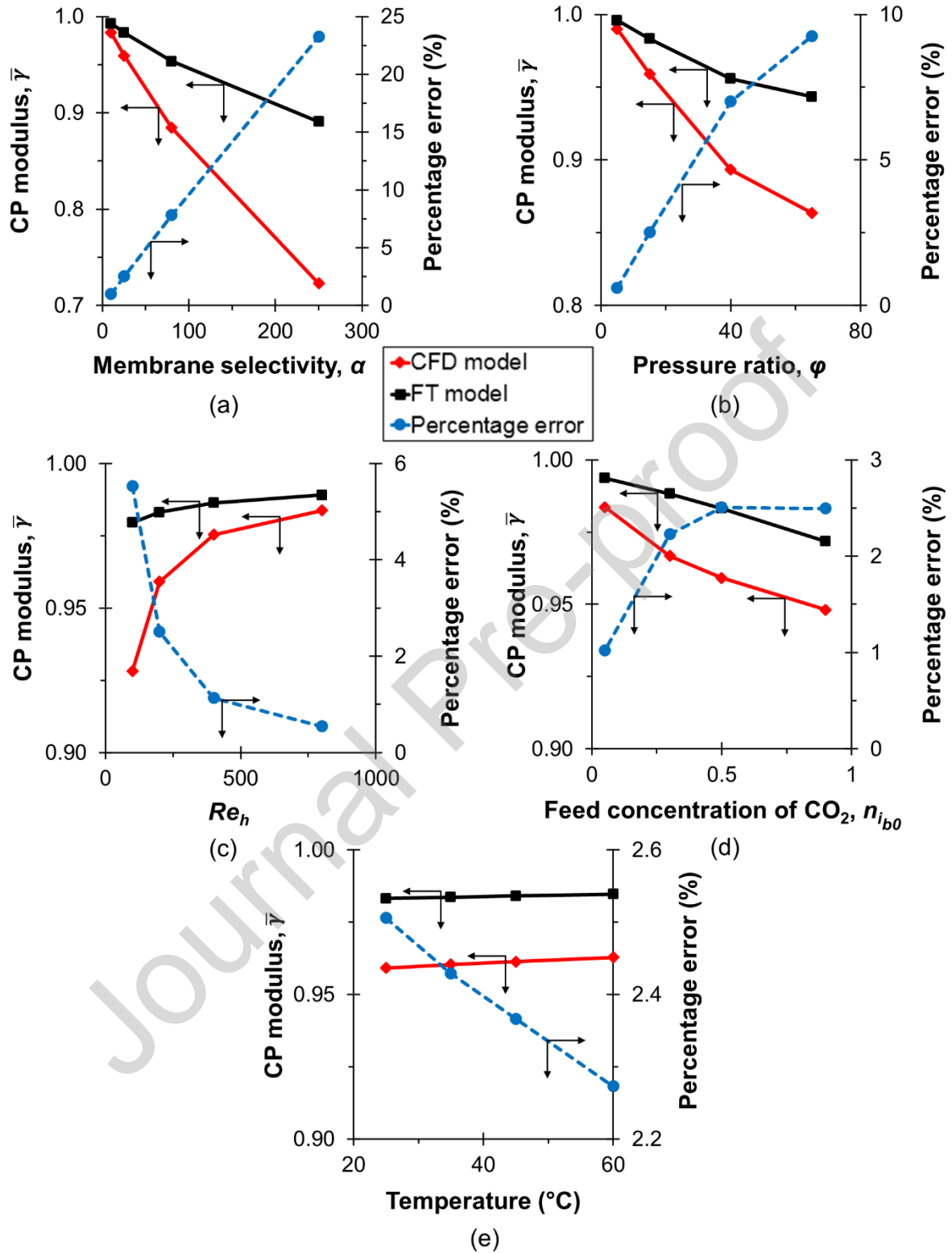


Figure 3: Effects of (a) membrane selectivity, (b) pressure ratio, (c) hydraulic Reynolds number, (d) feed composition, and (e) temperature on area-averaged modulus of concentration polarisation and prediction error (%) between analytical film theory (FT) and numerical (CFD) models.

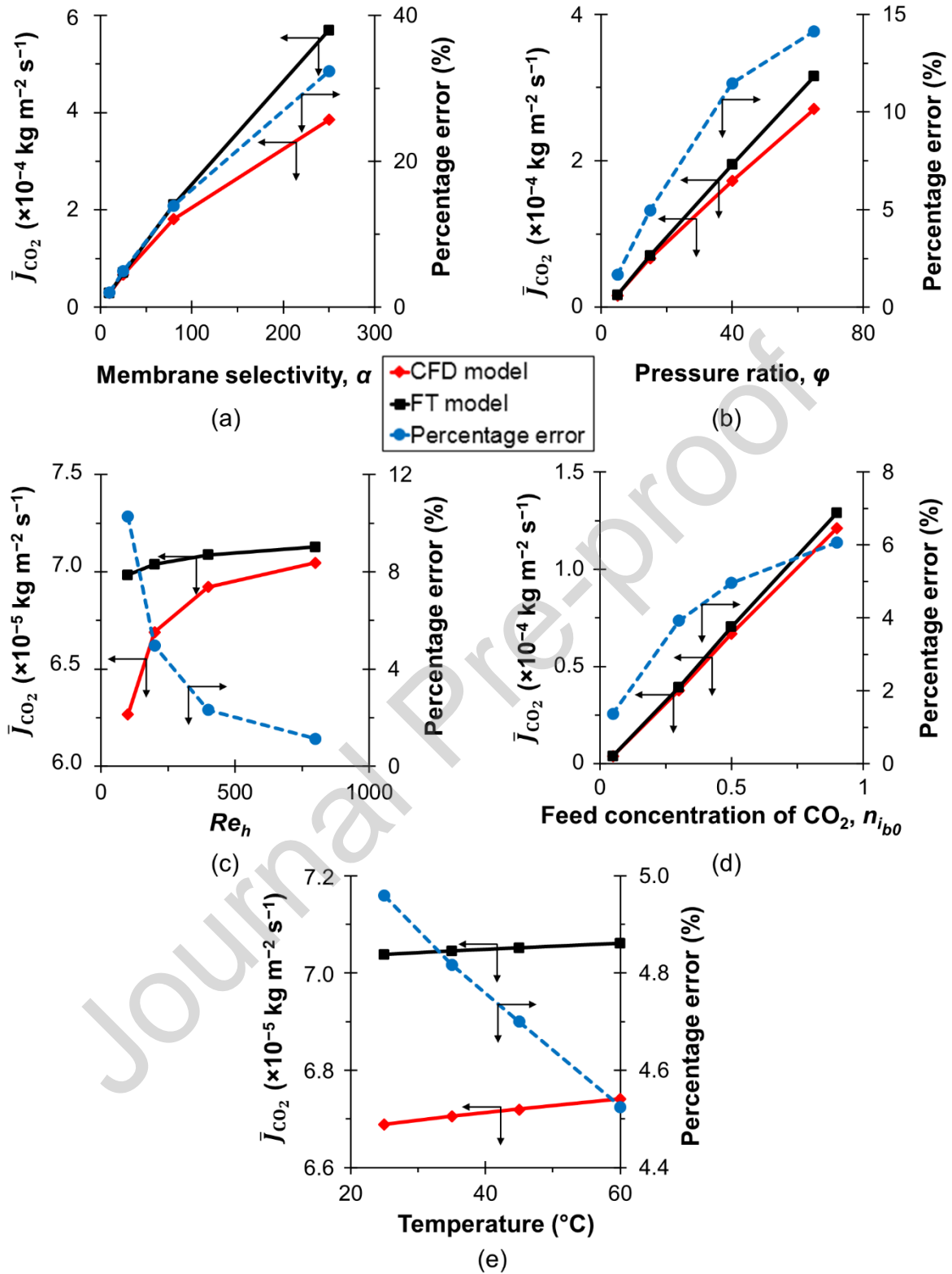


Figure 4: Effects of (a) membrane selectivity, (b) pressure ratio, (c) hydraulic Reynolds number, (d) feed composition, and (e) temperature on area-averaged permeate flux of CO₂ gas and prediction error (%) between analytical film theory (FT) and numerical (CFD) models.

3.2 Accuracy of analytical film theory in industrial membrane gas separation

In order to assess the accuracy of analytical film theory in industrial membrane gas separation, this section further compares the FT and CFD models across a series of operating variables, such as hydraulic Reynolds number, membrane selectivity, and pressure ratio that are typically encountered in industrial membrane processes. Table 6 lists the simulation parameters used for comparison between the models. A range of hydraulic Reynolds number (Re_h) from 100 to 800 is considered, which are typically applied in industrial gas separation membrane processes (Alkhamis et al., 2015; He, 2018). Given that the typical range of feed composition and temperature has little effect on CP and flux as mentioned in Section 3.1, a constant temperature of 25 °C and 0.5 mole fraction of feed gas concentration are used in this case.

Table 6: Simulation parameters used for comparison between FT and CFD models.

Case	1	2	3	4	5	6	7	8	9	10
Re_h	100	200	400	800	200	200	200	200	200	200
α	25	25	25	25	10	80	250	25	25	25
φ	15	15	15	15	15	15	15	5	40	65

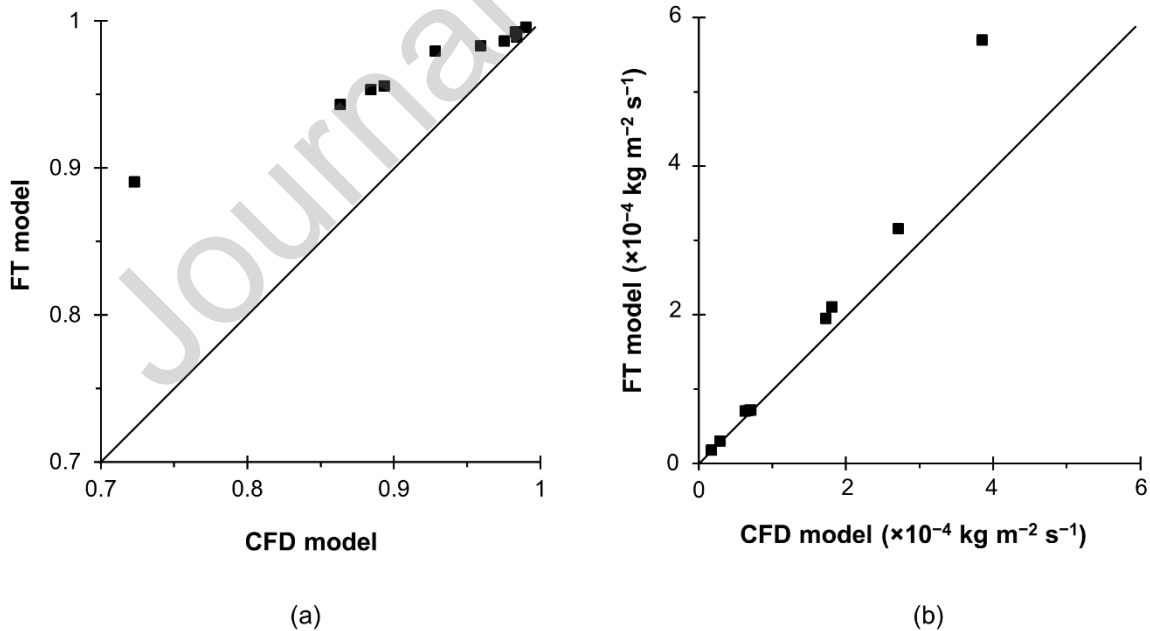


Figure 5: Comparison of predictions between analytical film theory (FT) and numerical (CFD) models for area-averaged (a) CP modulus and (b) CO₂ permeate flux. The temperature and feed concentration of CO₂ (mole fraction) are constant at 25 °C and 0.5, respectively for simulation conditions stated in Table 6.

Figure 5 shows the predictions of CP modulus and gas permeate flux by the FT model plotted against CFD results. It is found that there is an average difference of 5.2% in CP modulus predicted by both models as the FT model consistently underestimates CP, i.e., below 0.9 of CP modulus as shown in Figure 5a. This in turn causes the FT model to overestimate the CO₂ permeate flux and the difference becomes larger at fluxes higher than $2 \times 10^{-4} \text{ kg m}^{-2} \text{ s}^{-1}$, resulting in an average difference of 9.4% and a maximum deviation of 32.4% in flux predictions between the models (Figure 5b).

3.3 Estimation of local concentration polarisation by film theory

Accurate prediction of local CP becomes important in membrane gas separation process as significant CP phenomena would reduce gas permeation flux, thus decreasing the overall performance of membrane module. The local CP modulus (γ) can be estimated by using the analytical FT model and is expressed as

$$\gamma(x) = \frac{\exp(j_f(x) \cdot \delta(x) / D_i)}{1 + E_o [\exp(j_f(x) \cdot \delta(x) / D_i) - 1]} \quad (23)$$

where $j_f(x)$ is the local feed volumetric flux calculated by CFD model, and $\delta(x)$ is the local boundary layer thickness which can be obtained from equation (10).

Figure 6a shows that the difference in local γ predictions between the FT and CFD models decreases along the membrane channel at higher Re_h . This is because a higher Re_h enhances flow mixing and results in an increase in the boundary layer renewal near the membrane surface, which minimises CP in the membrane system, leading to a smaller difference in the local γ predictions between both models. Hence, a further increase in Re_h is expected to result in a closer prediction between the FT and CFD models in this case. Figure 6b and 6c, on the other hand, show that the difference in local γ predictions increases as membrane selectivity and/or pressure ratio increases. Overall, the trends obtained in Figure 6 show that the difference in local γ predicted between both models becomes larger along the membrane channel. This suggests that the CP prediction using the FT model is more reliable in the region closer to the entrance of membrane channel.

It should be noted that although this study is performed for typical CO₂/CH₄ gas separation, the insights drawn from this work are applicable to all gases as the mass transfer finding is driven by hydrodynamics, rather than the gas species. Nevertheless, for other gas

separation applications such as membrane gas absorption, the current CFD model should consider additional parameters such as the reaction rate of gas species along the membrane module. This is because membrane gas absorption involves both the gas permeation mechanism through membrane, as well as the chemical reaction of gas species in the absorption process.

Journal Pre-proof

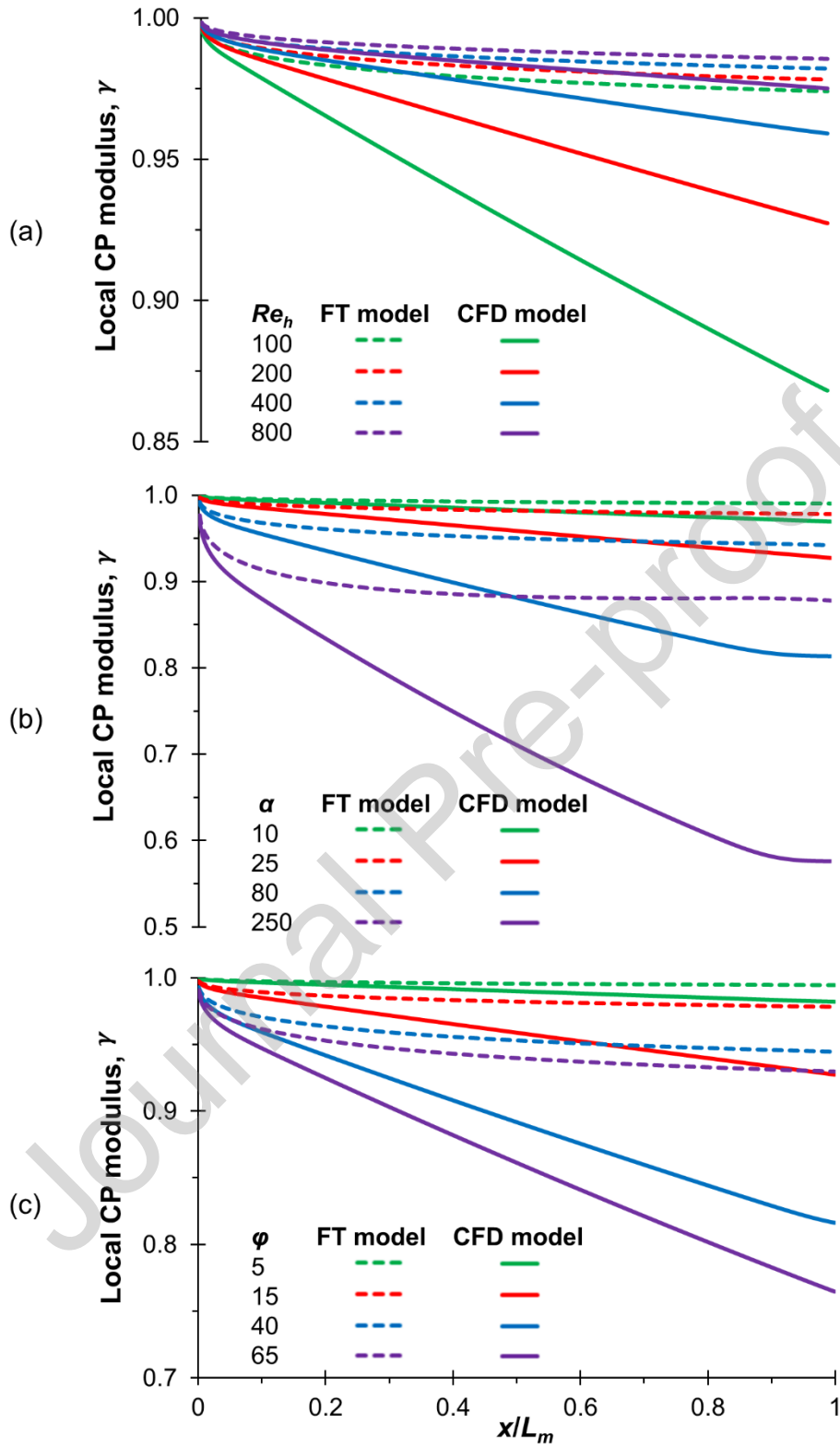


Figure 6: Effects of (a) hydraulic Reynolds number, (b) membrane selectivity, and (c) pressure ratio on local CP modulus estimated by analytical film theory (FT) and numerical (CFD) models along the membrane channel.

4 Conclusion

A comparative study of film theory against the numerical approach by CFD was performed for predicting concentration polarisation and flux performance in membrane gas separation. This study shows that the film theory model becomes less accurate typically at high CP conditions when gas permeation increases across the membrane due to higher membrane selectivity and pressure ratio, leading to a large difference in CP predictions as well as flux performance. This suggests that the film theory is not recommended for membranes with high permeance or high-pressure conditions. Given that the typical range of feed composition and temperature has little impact on fluid properties, both film theory and CFD models predict CP and flux performance similarly. Overall, the analytical film theory can serve as a reliable approximation for membrane gas applications under low CP at high crossflow and low flux conditions. The results also indicate that film theory is most accurate in predicting CP in the region closer to the membrane entrance. Although this study is performed for the most widely studied CO₂/CH₄ gas separation, the same insights could be applied to other similar gas applications for process design improvement in dense membrane modules.

Acknowledgements

The authors would like to acknowledge the funding support provided by Universiti Malaysia Pahang research grant (Reference code: PGRS1903134). One of us (K.F.) gratefully acknowledges the scholarship funding provided by Universiti Malaysia Pahang (UMP).

Nomenclature

Symbol

D	Diffusion coefficient (m ² s ⁻¹)
d_h	Hydraulic diameter (m)
E_o	Enrichment term
$f = \frac{d_h \Delta p_{ch}}{2 \rho u_{avg}^2 L_m}$	Fanning friction factor
h	Channel half-height (m)
h_{ch}	Membrane channel height (m)
j	Volumetric flux per unit area (m ³ m ⁻² s ⁻¹)

J	Mass flux ($\text{kg m}^{-2} \text{s}^{-1}$)
L_{in}	Entrance length (m)
L_m	Membrane length (m)
L_{out}	Exit length (m)
M	Molecular weight (g mol^{-1})
n	Mole fraction
p	Pressure (Pa)
P	Gas permeance ($\text{mol m}^{-2} \text{s}^{-1} \text{Pa}^{-1}$)
R	Ideal gas constant ($\text{atm L mol}^{-1} \text{K}^{-1}$)
$Re_h = \frac{\rho u_{avg} d_h}{\mu}$	Hydraulic Reynolds number
Sc	Schmidt number
t	Time (s)
T	Temperature ($^{\circ}\text{C}$)
u_{avg}	Average velocity (m s^{-1})
u_{b0}	Inlet velocity at any y-direction (m s^{-1})
v_w	Fluid velocity normal to the wall (m s^{-1})
\vec{v}	Velocity vector (m s^{-1})
w	Mass fraction
w_{ch}	Membrane channel width (m)
x	Distance in the bulk flow direction, parallel to membrane surface (m)
y	Distance from the bottom membrane surface, in direction normal to the surface (m)
<i>Greek letters</i>	
α	Membrane selectivity
δ	Film layer thickness (m)
γ	Concentration polarisation modulus
μ	Dynamic viscosity ($\text{kg m}^{-1} \text{s}^{-1}$)
φ	Pressure ratio
ρ	Density (kg m^{-3})
τ	Wall shear stress (Pa)

Subscript

<i>b</i>	Value at inlet bulk conditions
<i>f</i>	Value for the feed
<i>max</i>	Value for maximum variable
<i>mix</i>	Value for a binary gas mixture of CO ₂ and CH ₄
<i>o</i>	Value on the feed side membrane surface (wall)
<i>out</i>	Value at the domain outlet
<i>p</i>	Value for the permeate

List of Figures

Figure 1: Schematic diagram of CFD fluid domain (not to scale) for modelling of a gas separation feed channel.

Figure 2: Effect of hydraulic Reynolds number on Fanning friction factor and prediction error (%) between CFD model and analytical correlation.

Figure 3: Effects of (a) membrane selectivity, (b) pressure ratio, (c) hydraulic Reynolds number, (d) feed composition, and (e) temperature on area-averaged modulus of concentration polarisation and prediction error (%) between analytical film theory (FT) and numerical (CFD) models.

Figure 4: Effects of (a) membrane selectivity, (b) pressure ratio, (c) hydraulic Reynolds number, (d) feed composition, and (e) temperature on area-averaged permeate flux of CO₂ gas and prediction error (%) between analytical film theory (FT) and numerical (CFD) models.

Figure 5: Comparison of predictions between analytical film theory (FT) and numerical (CFD) models for area-averaged (a) CP modulus and (b) CO₂ permeate flux. The temperature and feed concentration of CO₂ (mole fraction) are constant at 25 °C and 0.5, respectively for simulation conditions stated in Table 6.

Figure 6: Effects of (a) hydraulic Reynolds number, (b) membrane selectivity, and (c) pressure ratio on local CP modulus estimated by analytical film theory (FT) and numerical (CFD) models along the membrane channel.

List of Tables

Table 1: Mathematical formulation used for estimation of gas mixture properties.

Table 2: Summary of the differences between the numerical approach and the film theory approximation.

Table 3: Mathematical expressions for boundary conditions of CFD model at different locations.

Table 4: Reference parameters used for gas separation case studies.

Table 5: Operating variables used for CO₂/CH₄ gas separation case studies.

Table 6: Simulation parameters used for comparison between FT and CFD models.

5 References

- Ahmad, F., Lau, K.K., Lock, S.S.M., Rafiq, S., Khan, A.U., Lee, M., 2015. Hollow fiber membrane model for gas separation: Process simulation, experimental validation and module characteristics study. *Journal of Industrial and Engineering Chemistry* 21, 1246-1257.
- Al-Obaidi, M.A., Mujtaba, I.M., 2016. Steady state and dynamic modeling of spiral wound wastewater reverse osmosis process. *Computers & Chemical Engineering* 90, 278-299.
- Alkhamis, N., Oztekin, D.E., Anqi, A.E., Alsaiari, A., Oztekin, A., 2015. Numerical study of gas separation using a membrane. *International Journal of Heat and Mass Transfer* 80, 835-843.
- Baker, R.W., 2004. *Membrane Technology and Applications*. John Wiley & Sons Ltd, England.
- Bhattacharya, S., Hwang, S.-T., 1997. Concentration polarization, separation factor, and Peclet number in membrane processes. *Journal of Membrane Science* 132, 73-90.
- Bird, R.B., Stewart, W.E., Lightfoot, E.N., 1960. *Transport Phenomena*. John Wiley & Sons, New York.
- Blinova, N.V., Svec, F., 2012. Functionalized polyaniline-based composite membranes with vastly improved performance for separation of carbon dioxide from methane. *Journal of Membrane Science* 423-424, 514-521.
- Brian, P.L.T., 1965. Concentration Polarization in Reverse Osmosis Desalination with Variable Flux and Incomplete Salt Rejection. *Industrial & Engineering Chemistry Fundamentals* 4, 439-445.
- Cakal, U., Yilmaz, L., Kalipcilar, H., 2012. Effect of feed gas composition on the separation of CO₂/CH₄ mixtures by PES-SAPO 34-HMA mixed matrix membranes. *Journal of Membrane Science* 417-418, 45-51.
- Chen, W.-H., Syu, W.-Z., Hung, C.-I., 2011. Numerical characterization on concentration polarization of hydrogen permeation in a Pd-based membrane tube. *International Journal of Hydrogen Energy* 36, 14734-14744.
- Chen, W.-H., Syu, W.-Z., Hung, C.-I., Lin, Y.-L., Yang, C.-C., 2012. A numerical approach of conjugate hydrogen permeation and polarization in a Pd membrane tube. *International Journal of Hydrogen Energy* 37, 12666-12679.
- Cussler, E.L., 1997. *Diffusion, Mass Transfer in Fluid Systems*, 2nd Edition ed. The Press Syndicate of the University of Cambridge, United Kingdom.
- Feng, F., Liang, C.-Z., Wu, J., Weber, M., Maletzko, C., Zhang, S., Chung, T.-S., 2021. Polyphenylsulfone (PPSU)-Based Copolymeric Membranes: Effects of Chemical Structure and Content on Gas Permeation and Separation. *Polymers* 13, 2745.
- Fimbres-Weihs, G.A., Wiley, D.E., 2010. Review of 3D CFD modeling of flow and mass transfer in narrow spacer-filled channels in membrane modules. *Chemical Engineering and Processing: Process Intensification* 49, 759-781.
- Fletcher, D.F., Wiley, D.E., 2004. A computational fluids dynamics study of buoyancy effects in reverse osmosis. *Journal of Membrane Science* 245, 175-181.
- He, G., Mi, Y., Lock Yue, P., Chen, G., 1999. Theoretical study on concentration polarization in gas separation membrane processes. *Journal of Membrane Science* 153, 243-258.
- He, X., 2018. A review of material development in the field of carbon capture and the application of membrane-based processes in power plants and energy-intensive industries. *Energy, Sustainability and Society* 8, 34.
- Huang, Y., Merkel, T.C., Baker, R.W., 2014. Pressure ratio and its impact on membrane gas separation processes. *Journal of Membrane Science* 463, 33-40.

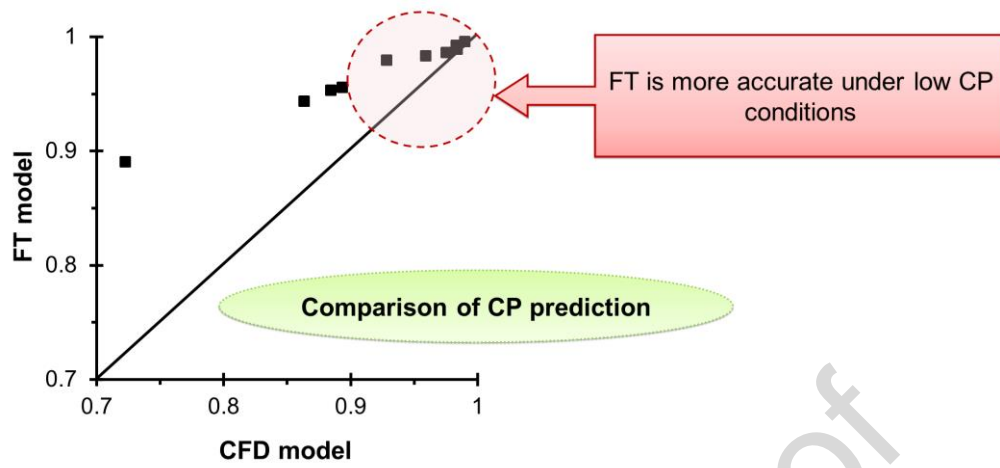
- Liang, C.Z., Liu, J.T., Lai, J.-Y., Chung, T.-S., 2018. High-performance multiple-layer PIM composite hollow fiber membranes for gas separation. *Journal of Membrane Science* 563, 93-106.
- Liang, C.Z., Yong, W.F., Chung, T.-S., 2017. High-performance composite hollow fiber membrane for flue gas and air separations. *Journal of Membrane Science* 541, 367-377.
- Liang, Y.Y., Chapman, M.B., Fimbres-Weihs, G.A., Wiley, D.E., 2014. CFD modelling of electro-osmotic permeate flux enhancement on the feed side of a membrane module. *Journal of Membrane Science* 470, 378-388.
- Liang, Y.Y., Fimbres-Weihs, G.A., Setiawan, R., Wiley, D.E., 2016. CFD modelling of unsteady electro-osmotic permeate flux enhancement in membrane systems. *Chemical Engineering Science* 146, 189-198.
- Lüdtke, O., Behling, R.D., Ohlrogge, K., 1998. Concentration polarization in gas permeation. *Journal of Membrane Science* 146, 145-157.
- Matthiasson, E., Sivik, B., 1980. Concentration polarization and fouling. *Desalination* 35, 59-103.
- Michaels, A.S., 1968. New separation technique for the CPI. *Chemical Engineering Progress* 64, 31-42.
- Moran, M.J., Shapiro, H.N., 1988. *Fundamentals of engineering thermodynamics*. John Wiley and Sons Inc., New York, NY, United States.
- Mourgues, A., Sanchez, J., 2005. Theoretical analysis of concentration polarization in membrane modules for gas separation with feed inside the hollow-fibers. *Journal of Membrane Science* 252, 133-144.
- Perry, R., Green, D., 2007. *Perry's chemical engineers' handbook*, 8th illustrated ed. New York: McGraw-Hill.
- Probstein, R.F., 1989. *Physicochemical Hydrodynamics: An Introduction*. John Wiley & Sons, Hoboken, New Jersey.
- Probstein, R.F., Shen, J.S., Leung, W.F., 1977. Ultrafiltration of macromolecular solutions at high polarization in laminar channel flow. *Desalination* 24, 1-16.
- Roache, P.J., Knupp, P.M., 1993. Completed Richardson extrapolation. *Communications in Numerical Methods in Engineering* 9, 365-374.
- Saedi, S., Madaeni, S.S., Hassanzadeh, K., Shamsabadi, A.A., Laki, S., 2014. The effect of polyurethane on the structure and performance of PES membrane for separation of carbon dioxide from methane. *Journal of Industrial and Engineering Chemistry* 20, 1916-1929.
- Schwinge, J., Wiley, D.E., Fletcher, D.F., 2002a. Simulation of the Flow around Spacer Filaments between Channel Walls. 2. Mass-Transfer Enhancement. *Industrial & Engineering Chemistry Research* 41, 4879-4888.
- Schwinge, J., Wiley, D.E., Fletcher, D.F., 2002b. Simulation of the Flow around Spacer Filaments between Narrow Channel Walls. 1. Hydrodynamics. *Industrial & Engineering Chemistry Research* 41, 2977-2987.
- Takaba, H., Nakao, S.-i., 2005. Computational fluid dynamics study on concentration polarization in H₂/CO separation membranes. *Journal of Membrane Science* 249, 83-88.
- White, L.S., Blinka, T.A., Kloczewski, H.A., Wang, I.f., 1995. Properties of a polyimide gas separation membrane in natural gas streams. *Journal of Membrane Science* 103, 73-82.
- Wiley, D.E., Fletcher, D.F., 2003. Techniques for computational fluid dynamics modelling of flow in membrane channels. *Journal of Membrane Science* 211, 127-137.
- Wilke, C.R., 1950. A Viscosity Equation for Gas Mixtures. *The Journal of Chemical Physics* 18, 517-519.
- Yu, L., Nobandegani, M.S., Hedlund, J., 2022. Industrially relevant CHA membranes for CO₂/CH₄ separation. *Journal of Membrane Science* 641, 119888.

Zhang, J., Liu, D., He, M., Xu, H., Li, W., 2006. Experimental and simulation studies on concentration polarization in H₂ enrichment by highly permeable and selective Pd membranes. *Journal of Membrane Science* 274, 83-91.

Zydney, A.L., 1997. Stagnant film model for concentration polarization in membrane systems. *Journal of Membrane Science* 130, 275-281.

Journal Pre-proof

Graphical abstract



Journal Pre-proof

Declaration of interests

The authors declare that they have no known competing financial interests or personal relationships that could have appeared to influence the work reported in this paper.

The authors declare the following financial interests/personal relationships which may be considered as potential competing interests:

Journal Pre-proof

Highlights

- Comparison of CP predicted by film theory and CFD model for membrane gas separation
- Fluid properties have little impact on CP and flux predicted by FT and CFD models
- Film theory performs better in the region closer to the membrane entrance
- FT predictions are at their best for high crossflow and low flux conditions

Journal Pre-proof